

CEBPB-high dormant tumor cells drive immune evasion via S100A8 orchestrated tumor-associated macrophages reprogramming

Jin Bai ^{1,2}, Huilan Su ³, Shunxi Wang^{4,5*}, Yang Dong ^{3,4*}, Yong Gao ^{1*}

Affiliation

1 Department of Oncology, Shanghai East Hospital, Tongji University School of Medicine, 150 Jimo Road, Pudong District, Shanghai, 200120, China.

2 Cancer Center of Daping Hospital, Army Medical University, Chongqing, 400037, China.

3 Research Center for Translational Medicine, Cancer Stem Cell Institute, Shanghai East Hospital, Tongji University School of Medicine, 150 Jimo Road, Pudong District, Shanghai, 200120, China.

4 Institute of Pathology and Southwest Cancer Center, Southwest Hospital, Third Military Medical University (Army Medical University), and The Key Laboratory of Tumor Immunopathology, The Ministry of Education of China, Chongqing, 400038, P.R. China

5 Chongqing Institute of Advanced Pathology, Jinfeng Laboratory, Chongqing, 400039.China

*Corresponding author

Yong Gao (drgaoyong@tongji.edu.cn)

Yang Dong (1810441@tongji.edu.cn)

Shunxi Wang (sx_wang1024@126.com)

Supplementary Figures

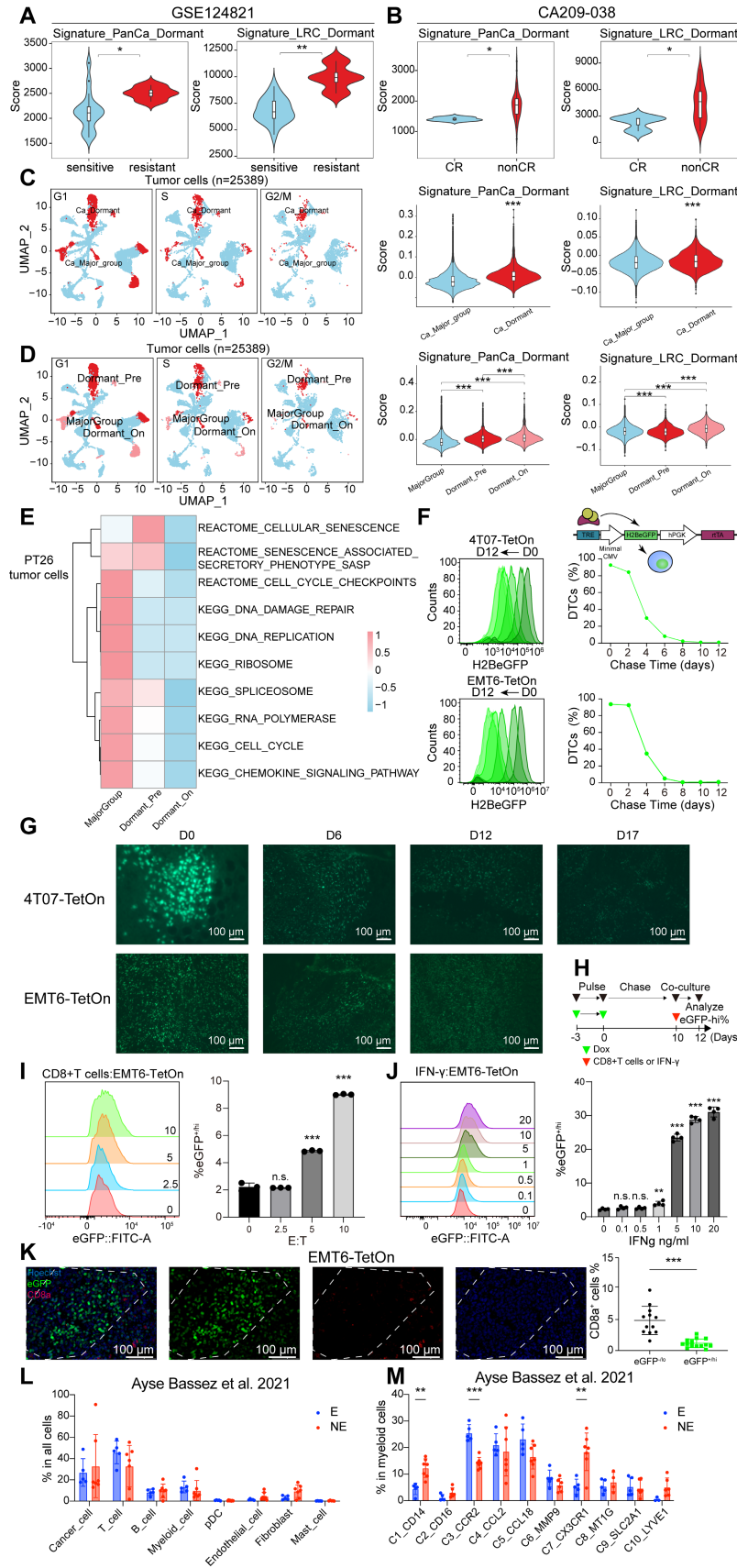


Figure S1. Dormant tumor cells occupy an immunosuppressive niche and mediate ICB resistance in TNBC.

A-B, Violin plots showing expression scores of Signature_LRC_Dormant and Signature_PanCa_Dormant in GSE124821 and RNA-seq data of the CA209-038 study.

C, Umap plots of cell cycle score analysis categorizing 25389 tumor cells from the all 12 TNBC patients into Dormant and MajorGroup clusters (Left). Violin plots showing expression scores of Signature_LRC_Dormant and Signature_PanCa_Dormant in these clusters (Right).

D, Umap plots of cell cycle score analysis categorizing 25389 tumor cells from the all 12 TNBC patients into Dormant_Pre, Dormant_On, and MajorGroup clusters (Left). Violin plots showing expression scores of Signature_LRC_Dormant and Signature_PanCa_Dormant in these clusters (Right).

E, GSVA analysis of tumor cell clusters from PT26 patient.

F, Label retention effect of TetOn-H2BeGFP system on 4T07 and EMT6 cells cultured in vitro. 4T07-TetOn and EMT6-TetOn cells were cultured in doxycycline (DOX) -containing medium (5 $\mu\text{g}/\text{mL}$) for 3 days (pulsing), followed by passaging in DOX-free medium for 12 days (chasing). Cells were collected every 2 days, and the proportion of cells retaining eGFP fluorescence was analyzed using flow cytometry (left). Fluorescence retention curves for the 12-day chase period were also generated (right), demonstrating that after 8-12 days of chasing, only approximately 1% of the cells retained elevated levels of eGFP fluorescence, thereby identifying them as dormant tumor cells.

G, The TetOn-H2BeGFP system demonstrated the labeling retention effect in the in vivo tumors. The retention of eGFP fluorescence in 4T07-TetOn and EMT6-TetOn allografts were assessed using fluorescence microscopy.

H, Experimental model diagram of T cell or IFN- γ mediated killing assay.

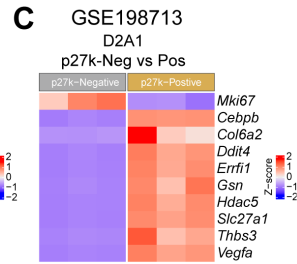
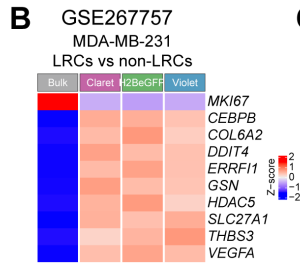
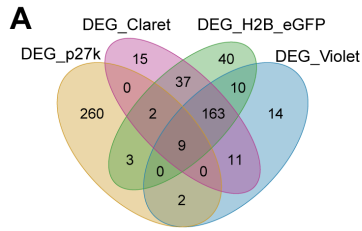
I, T cell cytotoxicity assay. CD8⁺ T cells from OT-1 mice were co-cultured with EMT6-TetOn-OVA cells that had been labeled with DOX and tracked for 10 days at varying effector to target ratios (E:T) for 48 hours.

J, IFN- γ cytotoxicity assay, EMT6-TetOn cells labeled with doxycycline and tracked for 10 days were treated with different concentrations of IFN- γ for 48 hours. The proportion of eGFP^{+/_{high}} cells was analyzed using flow cytometry.

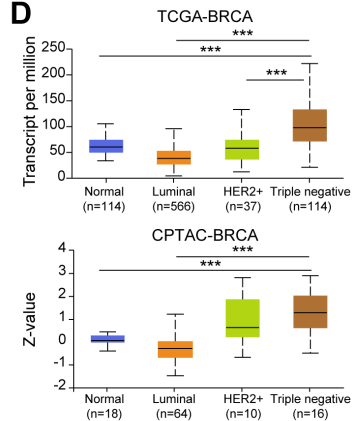
K, Representative IF plots of CD8a staining in EMT6-TetOn serial tumor sections. White dashed line marks eGFP^{+/_{high}} area.

L, The percentage of major cell subpopulation refers to its proportion out of the patient's total cells from a cohort of 12 TNBC patients in the scRNA-seq dataset published by Ayse Bassez et al., categorized into clonotype expansion (E, blue) and no/limited expansion (NE, red) groups based on T cell clone expansion following anti-PD-1 therapy.

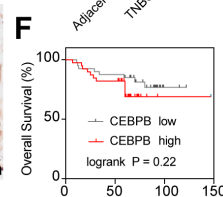
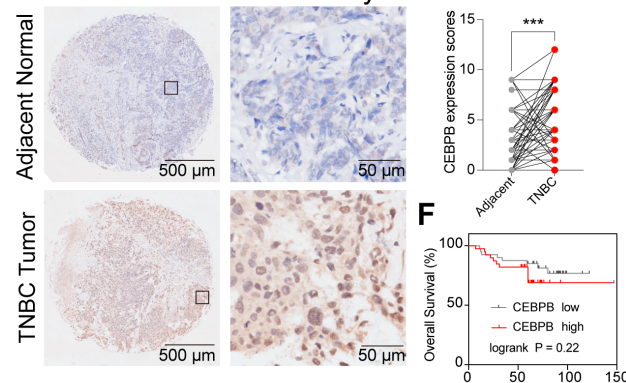
M, The percentage of macrophage subpopulation refers to its proportion out of the patient's main macrophage count from a cohort of 12 TNBC patients in the scRNA-seq dataset published by Ayse Bassez et al., categorized into clonotype expansion (E, blue) and no/limited expansion (NE, red) groups based on T cell clone expansion following anti-PD-1 therapy. n.s, not significant, *, $P < 0.05$, **, $P < 0.01$, ***, $P < 0.001$.



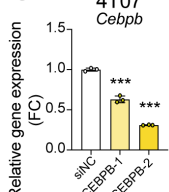
D CEBPB level in breast cancer



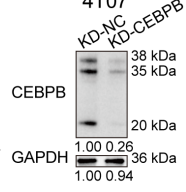
E TNBC-tissue microarray



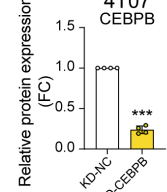
G 4T07 Cebpb



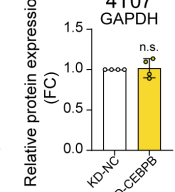
H 4T07



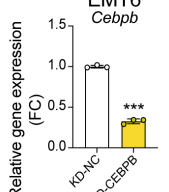
I 4T07 CEBPB



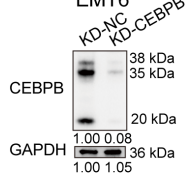
J 4T07



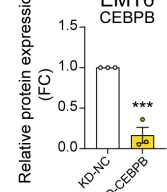
K BALB/c-nude EMT6



L BALB/c-nude EMT6



M BALB/c-nude EMT6



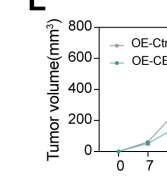
N 4T07 OE-CEBPB



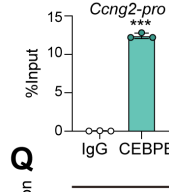
O 4T07-OE-Ctrl 4T07-OE-CEBPB



P EMT6-OE-Ctrl EMT6-OE-CEBPB



Q 4T07



R EMT6

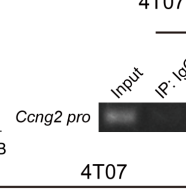


Figure S2. CEBPB as an essential factor in the tumor dormancy of TNBC Cells.

A, Venn diagram showing the upregulated genes in dormant TNBC cells identified from GSE267757 and GSE198713.

B-C, Heatmaps showing the 9 common upregulated genes and *Ki67* mRNA expression in GSE267757 (B) and GSE198713 (C).

D, boxplot of CEBPB expression levels across different breast cancer subtypes from TCGA-BRCA and CPTAC-BRCA.

E, Representative immunohistochemistry images of CEBPB staining in a TMA with adjacent normal samples and TNBC tumor samples ($n = 80$ per group), and the expression of CEBPB protein in the two groups was statistically analyzed.

F, Kaplan-Meier analysis (log-rank test) of CEBPB expression in tumor samples of the TNBC-TMA. Median expression of CEBPB was as the group cutoff ($n = 40$ per group).

G, mRNA expression of *Cebpb* in 4T07 cells transfected with the siCEBPB-1 and siCEBPB-2. The siCEBPB-2 sequence was selected to construct the KD-CEBPB lentivirus vector. And mRNA expression of *Cebpb* in EMT6 KD-CEBPB cells.

H-I, Protein expression of CEBPB in 4T07 KD-CEBPB and EMT6 KD-CEBPB cells.

J, Cell viability assessed by Cell Counting Kit-8 assay in 4T07 and EMT6 cells with or without CEBPB knockdown.

K-M, Tumor image (K), volume (L) and weight (M) of EMT6 OE-CEBPB allografts in BALB/nude mice ($n = 5$).

N-P, ChIP-qPCR (N) and DNA gel electrophoresis (O-P) showing the CEBPB binding region in the promoter regions of *Ccng2* of 4T07 and EMT6 cells with or without CEBPB overexpression.

Q, Corresponding statistic data of Figure2M. *, $P < 0.05$, **, $P < 0.01$, ***, $P < 0.001$.

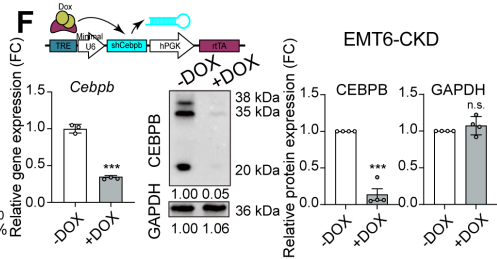
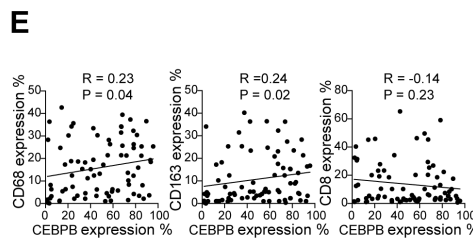
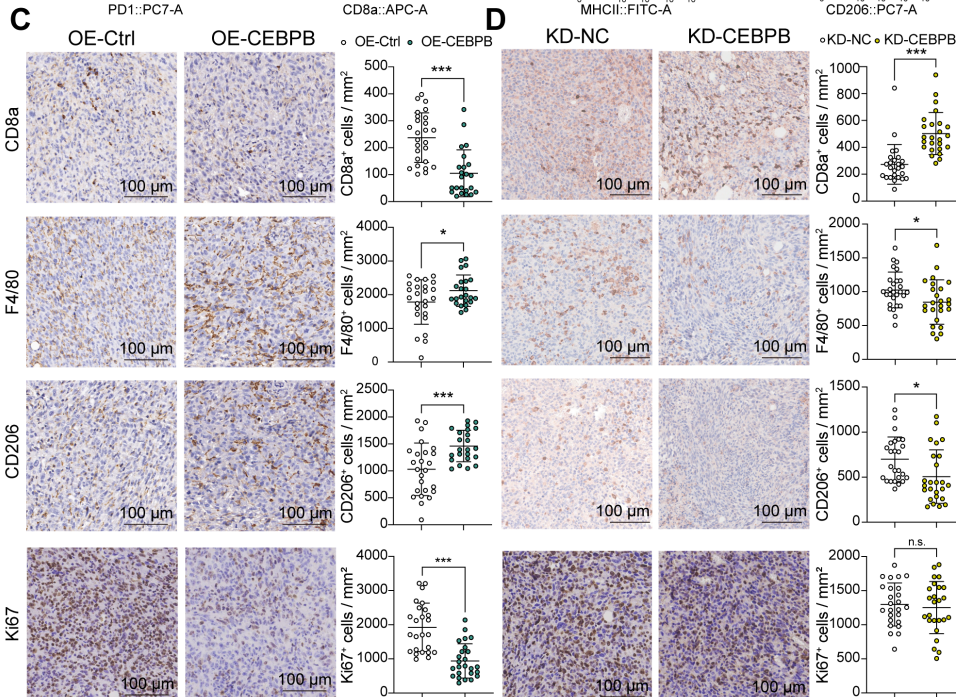
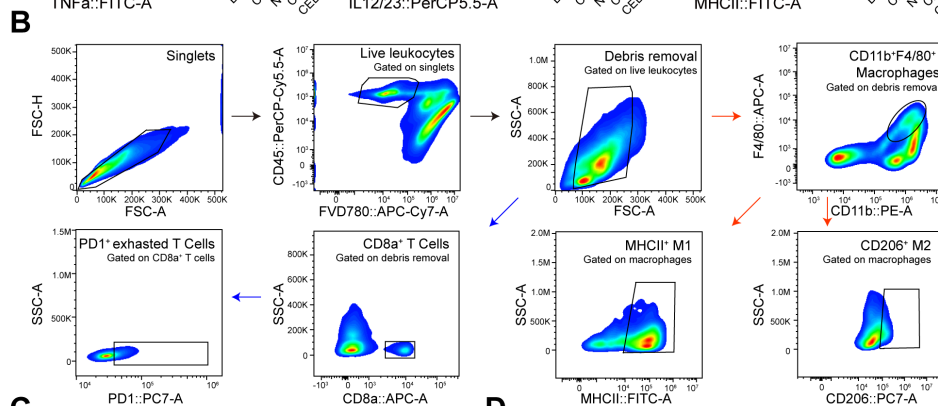
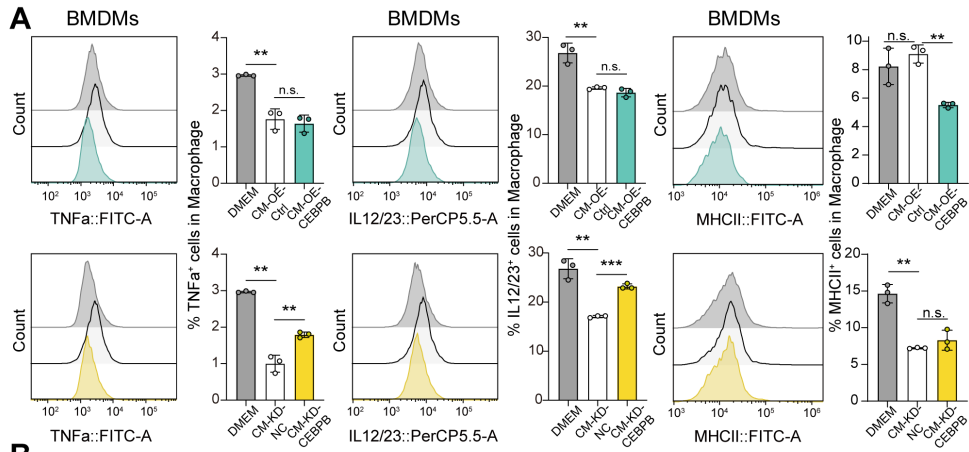


Figure S3. Highly expressed CEBPB tumors facilitate a tumor-promoting phenotype in TNBC.

A, Percentages of TNF α , IL12/23 and MHC II expressing BMDM co-cultured with CM from 4T07 with CEBPB overexpression or knockdown.

B, Gating strategy for tumor infiltrating immune cells

C-D, Representative immunohistochemistry images of CD8a, F4/80, CD206 and Ki67 staining in serial tumor sections of EMT6 allografts from CEBPB overexpression (C) or knockdown (D).

E, Scatter plots showing correlation analyses between percentages of CEBPB expression (x-axis) and percentages of immune cell infiltration markers CD68, CD163 and CD8 expression (y-axis) in 80 tumor samples from a TNBC-TMA analyzed by multiplex immunohistochemistry.

F, CEBPB-CKD plasmid structure model diagram and mRNA expression, protein expression of CEBPB in EMT6-CKD cells. *, $P < 0.05$, ***, $P < 0.001$.

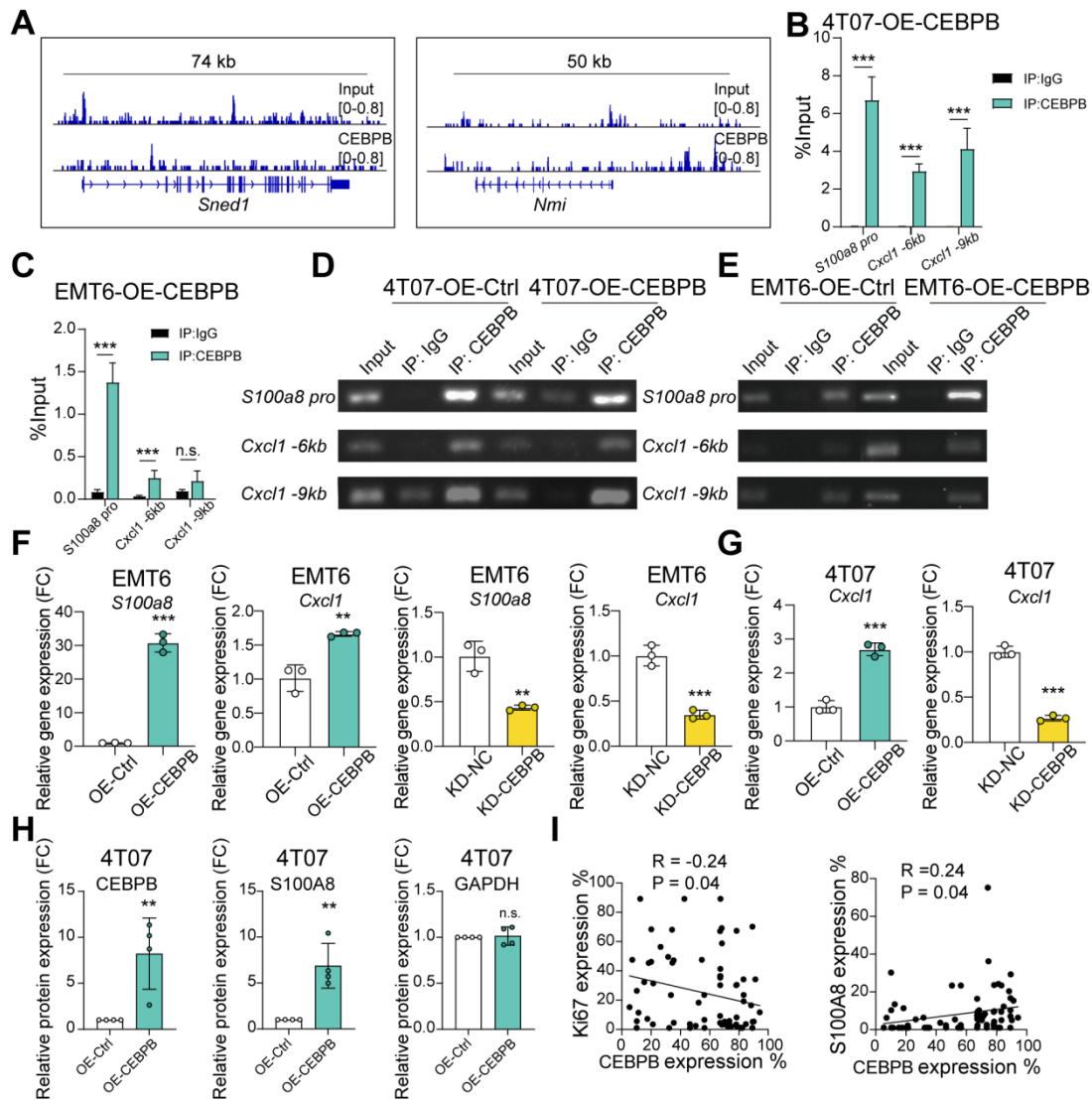


Figure S4. CEBPB transcriptionally activates S100A8 in TNBC.

A, CEBPB binding peaks for *Sned1* and *Nmi* from anti-CEBPB ChIP-seq in 4T07 cells. B-E, ChIP-qPCR (B-C) and DNA gel electrophoresis (D-E) showing the CEBPB binding regions in the *S100a8* promoter or upstream regions of *Cxcl1* of 4T07 and EMT6 cells with or without CEBPB overexpression.

F-G, mRNA expression of *S100a8* or *Cxcl1* in EMT6 (F) and 4T07 (G) cells with CEBPB overexpression or knockdown.

H, Corresponding statistic data of Figure 6G.

I, Scatter plots showing correlation analyses between percentages of CEBPB expression (x-axis) and Ki67, and S100A8 expression (y-axis) in 80 tumor samples from a TNBC-TMA analyzed by multiplex immunohistochemistry. n.s., not significant, * $P < 0.05$, ** $P < 0.01$, *** $P < 0.001$.

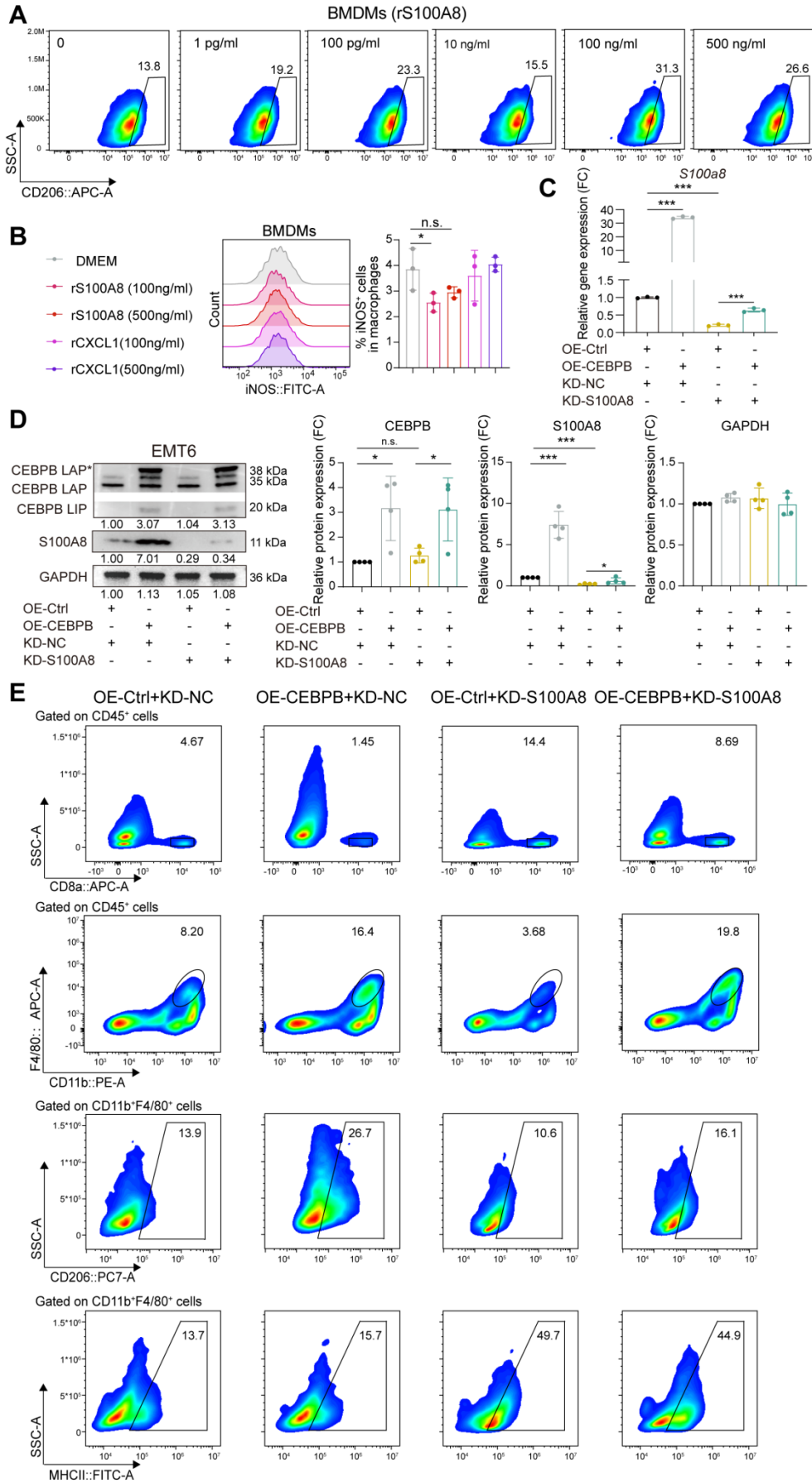


Figure S5. knockdown S100A8 reverses immune evasion caused by CEBPB overexpression in TNBC.

A, Percentages of CD206 expressing BMDMs with the addition of rS100A8 at varying concentrations for 48 hours.

B, Percentage of iNOS expressing BMDMs with the addition of rS100A8 (100 or 500 ng/mL) or rCXCL1 (100 or 500 ng/mL) for 48 hours.

C-D, mRNA (C) and Protein (D) expression of CEBPB and S100A8 in EMT6 cells with CEBPB overexpression and/or S100A8 knockdown.

E, Flow cytometry analysis of CD8⁺ T cells, CD11b⁺ F4/80⁺ cells, CD206⁺ macrophages, and MHCII⁺ macrophages infiltrated in tumors developed in CEBPB-overexpressing with or without S100A8 knockdown EMT6 allografts as in Figure 6L-R. *, $P < 0.05$, **, $P < 0.01$, ***, $P < 0.001$.

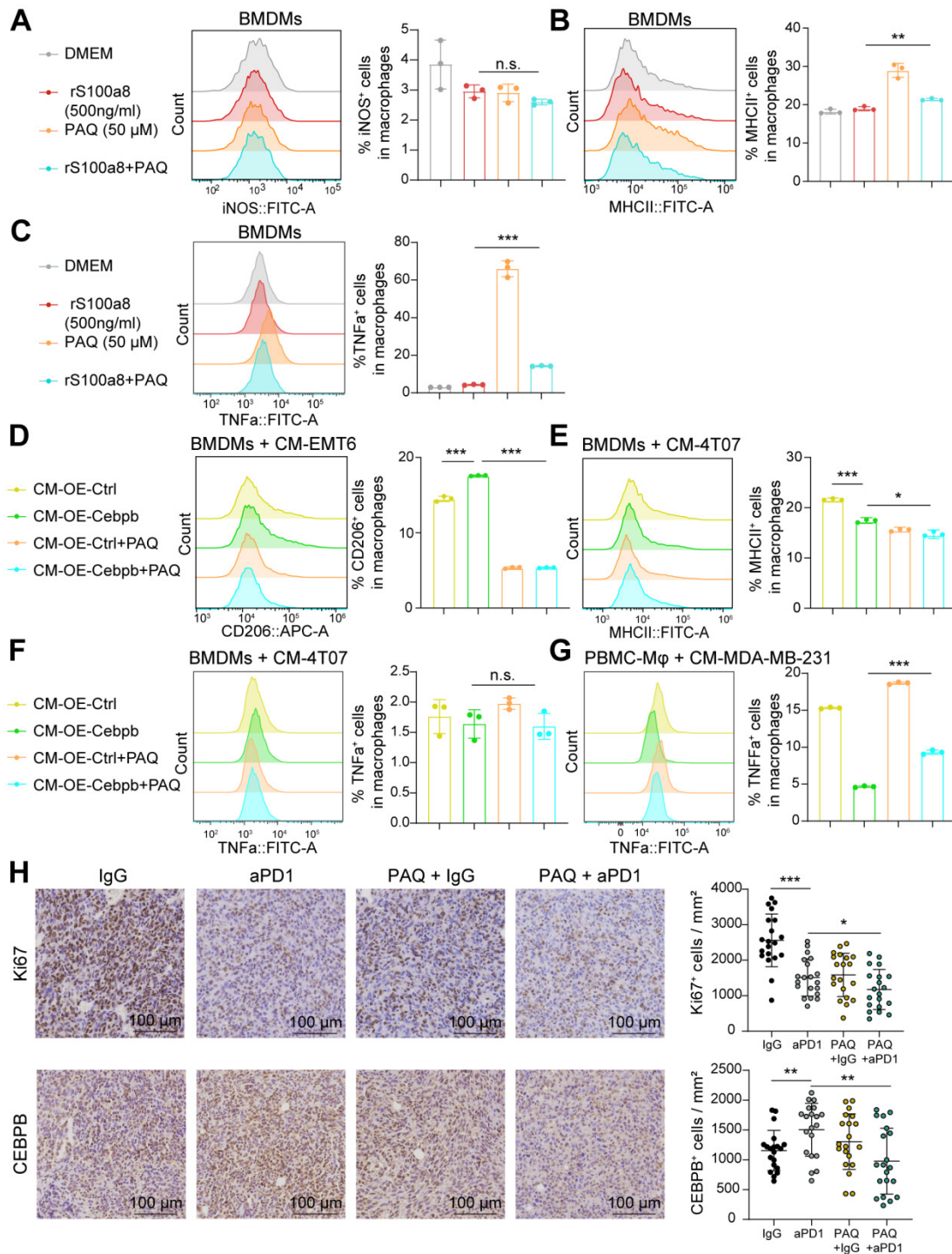


Figure S6. S100A8 inhibitor PAQ reverses macrophage M2 polarization caused by rS100a8 addition or CEBPB overexpression in TNBC.

A-C, Percentage of iNOS (A), MHC II (B) and TNFa (C) expressing BMDM with the addition of paquinimod (PAQ, 5 $\mu\text{g}/\text{mL}$) and/or rS100A8 (500 ng/mL) for 48 hours.

D, Percentages of CD206 expressing BMDM co-cultured with CM and/or PAQ (5 $\mu\text{g}/\text{mL}$) for 48 hours, including from EMT6 with or without CEBPB overexpression.

E, Percentages of MHCII expressing BMDM co-cultured with CM and/or PAQ (5 $\mu\text{g}/\text{mL}$) for 48 hours, including from 4T07 with or without CEBPB overexpression.

F-G, Percentages of TNFa expressing BMDM (F) or PMBC-M ϕ (G) co-cultured with CM and/or PAQ (5 $\mu\text{g}/\text{mL}$) for 48 hours, including from 4T07 (F) or MDA-MB-231 (G) with or without CEBPB overexpression.

H, Representative immunohistochemistry images of Ki67 and CEBPB staining in tumor sections of EMT6 allografts in Figure.7F-H. *, $P < 0.05$, **, $P < 0.01$, ***, $P < 0.001$.